ACADEMIC PRESS

Available online at www.sciencedirect.com

SCIENCE DIRECT®

Journal of Sound and Vibration 271 (2004) 147–158

JOURNAL OF SOUND AND VIBRATION

www.elsevier.com/locate/jsvi

Free vibrations of rectangular cantilever plates. Part 2: in-plane motion

Jongwon Seok*, H.F. Tiersten, H.A. Scarton

Department of Mechanical, Aerospace and Nuclear Engineering, Rensselaer Polytechnic Institute, 110 8th street, Troy, NY 12180-3590, USA

Received 9 May 2002; accepted 26 February 2003

Abstract

An analysis of the free in-plane vibrations of a cantilevered rectangular plate is performed by means of a variational approximation procedure. The problem is treated by first obtaining the exact solution for waves in the plate satisfying the equations of plane stress including in-plane inertia with two opposite edges traction free. The solution results in a set of dispersion curves. A number of the resulting waves are used in what remains of the variational equation, in which all conditions occur as natural conditions. Roots of the resulting transcendental equation are calculated, which yield the eigensolutions and associated eigenfrequencies. The results are compared with results obtained using FEM, and good agreement is shown.

1. Introduction

In this work, the equations of plane stress including in-plane inertia are used to treat the problem of the free vibrations of a thin relatively short cantilever plate. Although the results obtained from the analysis of the transverse vibration of a thin plate are available for a wide range of boundary conditions and aspect ratios, there is a paucity of results in the open literature regarding the in-plane motion of the plate. Kobayashi et al. [1] performed the calculation for the in-plane motion of such a plate with point supports. More recently, Bardell et al. [2] performed the eigenanalysis for the cases of all edges free and all edges clamped using the Rayleigh-Ritz method for the in-plane motion of isotropic rectangular plates.

*Corresponding author. Tel.: +1-518-276-8003; fax: +1-518-276-8761.
E-mail address: seokj@alum.rpi.edu (J. Seok).

0022-460X/03/$ - see front matter
doi:10.1016/S0022-460X(03)00366-3

Since the cantilever plate is short, the simple one-dimensional equations of the flexure of a beam will not yield accurate results. Since the problem of the in-plane free vibrations of a rectangular plate held at one edge and free on the other three cannot be solved exactly, it must be treated by some form of approximation procedure. A variational approximation procedure similar to that employed in Part 1 [3] is used, in which the differential equations and traction-free conditions on two opposite edges are satisfied exactly and the remaining conditions are satisfied by means of what remains in the variational equation. In the treatment, the variational equation of linear elastic plane stress with in-plane inertia is taken from Part 1. As in Part 1, all conditions, i.e., those of both natural and constraint types, arise as natural conditions in a form suitable for the application in this work. The analysis proceeds by satisfying the dynamic linear plane stress equations and the free edge conditions on two opposite faces exactly, while the remaining edge conditions are satisfied variationally.

The exact solution of the differential equations and free edge conditions on opposite faces yields dispersion curves. The dispersion curves for in-plane flexure of rectangular plates presented in this work are exact and, to our knowledge, have not appeared in the literature before. Up to seven of these solutions are taken, which are represented by the dispersion curves in what remains of the variational equation with all natural conditions to obtain a system of linear homogeneous algebraic equations, from which calculations are performed. Among other things, the calculation clearly reveals the dependence of the frequencies of free vibrations on the length-to-width ratio.

2. Variational equation for the in-plane motion of a thin orthotropic plate

Consider a fixed Cartesian co-ordinate system x_i with the faces, of area S, at $x_3 = \pm h$. The axes x_1 and x_2 are co-ordinates lying in the middle plane, which intersect the right prismatic boundary of the plate in a line path c. The origin of the x_2 co-ordinate axis is rigidly attached to the plate and the plate is bounded by a fixed edge at $x_1 = -l$ and three free edges at $x_1 = l$, $x_2 = \pm b$ (see Fig. 1). In this work as in Part 1 the material of the plate is taken to have orthotropic symmetry, in which the three-dimensional extensional constitutive equations are not coupled with

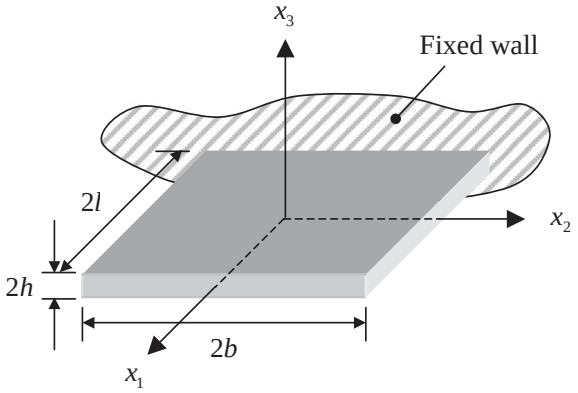

Fig. 1. A schematic of rectangular plate fixed on one edge and free on the other three.

the independent shear constitutive equations. In Part 1, the variational equation for both the extension and flexure of thin plates with all conditions arising as natural conditions was obtained from the appropriate three-dimensional variational equation [4].[1] In Part 1, the extensional behavior, which uncouples from the flexural behavior, was taken to vanish because only the transverse motion was treated. In this work the flexural behavior is taken to vanish and only the in-plane motion is treated. From (16) of Part 1, when the flexural motion is taken to vanish, there results

$$\int_{t_0}^{t} \mathrm{d}t\left[\int_S (\tau_{ab,a}^{(0)} - 2\rho h\ddot{u}_b^{(0)})\delta u_b^{(0)}\,\mathrm{d}S - \int_{c_N} n_a\tau_{ab}^{(0)}\delta u_b^{(0)}\,\mathrm{d}s + \int_{c_C} u_b^{(0)}\delta(n_a\tau_{ab}^{(0)})\,\mathrm{d}s\right] = 0, \tag{1}$$

where

$$\tau_{ab}^{(0)} = \int_{-h}^{h} \tau_{ab}\,\mathrm{d}x_3 \tag{2}$$

and the notation is defined in Section 2 of Part 1. Note that all of the inhomogeneous terms in Eq. (1) have been ignored since they are not required in this treatment. In this work, it is also assumed that the system obeys the linear constitutive equations and the infinitesimal strain–displacement gradient relations given in Eqs. (2) and (3) of Part 1.

From the assumption of plane stress and with the three-dimensional constitutive equations for the material having orthotropic symmetry, the two-dimensional constitutive equations for the lowest order extensional motion of the plate were obtained in Part 1. From Eqs. (7), (8), (14) and (15) of Part 1, there results

$$\tau_{11}^{(0)} = 2hc_{11}^{*}(u_{1,1}^{(0)} + \hat{v}u_{2,2}^{(0)}),\quad \tau_{22}^{(0)} = 2hc_{11}^{*}(Ru_{2,2}^{(0)} + \hat{v}u_{1,1}^{(0)}), \tag{3}$$

$$\tau_{12}^{(0)} = 2\,hc_{66}(u_{1,2}^{(0)} + u_{2,1}^{(0)}). \tag{4}$$

For the plate fixed on one edge and free on the other three shown in Fig. 1, the variational equation (1) takes the form

$$\begin{aligned}\int_S (\tau_{ab,a}^{(0)} - 2\rho h\ddot{u}_b^{(0)})\delta u_b^{(0)}\,\mathrm{d}S - \int_{-l}^{l} \mathrm{d}x_1[[n_a\tau_{ab}^{(0)}\delta u_b^{(0)}]_{x_2=-b} + [n_a\tau_{ab}^{(0)}\delta u_b^{(0)}]_{x_2=b}]\\ + \int_{-b}^{b} \mathrm{d}x_2[u_b^{(0)}\delta(n_a\tau_{ab}^{(0)})]_{x_1=-l} - \int_{-b}^{b} \mathrm{d}x_2[n_a\tau_{ab}^{(0)}\delta u_b^{(0)}]_{x_1=l} = 0,\end{aligned} \tag{5}$$

where the definition $[f(x)]_{x=p} = f(p)$ has been employed.

As discussed in Part 1, since in the formulation the constraint conditions were included by the method of Lagrange multipliers, each variation is treated as independent, the coefficient of each variation in Eq. (5) must vanish, which yields the differential equations and edge conditions. However, since the resulting equations cannot be solved exactly, this problem is treated by first satisfying exactly the differential equations and edge conditions on the two opposite traction-free edges. This solution yields dispersion relations. In the next section the dispersion relations of the

[1] Section 6.4 (6.44) without the electrical terms and the integral over $S^{(d)}$, since it is for only one region.

rectangular plate for the in-plane motion are obtained for the symmetric and antisymmetric modes, separately.

3. Solution of the differential equations and edge conditions on the two traction-free opposite faces

Since the $\delta u_b^{(0)}$ in the surface integral in Eq. (5) are independent, the differential equations for the in-plane motion of the plate take the well-known form

$$\tau_{ab,a}^{(0)} = 2\,\rho h \ddot{u}_b^{(0)}. \tag{6}$$

In addition, since the $\delta u_b^{(0)}$ at $x_2 = \pm b$ are independent, from Eq. (5), the edge conditions can be written in the form

$$\tau_{22}^{(0)} = 0, \quad \tau_{21}^{(0)} = 0 \quad \text{at } x_2 = \pm b. \tag{7}$$

The substitution of Eqs. (3) and (4) into Eq. (6) now yields

$$2h\{c_{11}^* u_{1,11}^{(0)} + (c_{11}^* \hat{\nu} + c_{66}) u_{2,12}^{(0)} + c_{66} u_{1,22}^{(0)}\} = 2\,\rho h \ddot{u}_1^{(0)}, \tag{8}$$

$$2h\{(c_{11}^* \hat{\nu} + c_{66}) u_{1,12}^{(0)} + c_{11}^* R u_{2,22}^{(0)} + c_{66} u_{2,11}^{(0)}\} = 2\rho h \ddot{u}_2^{(0)}, \tag{9}$$

which are the in-plane equations of motion of the thin plate. A solution of the coupled Eqs. (8) and (9) can be written in the form

$$u_1^{(0)} = A_1 \cos(\gamma x_1)\sin(\varsigma x_2 + s')\mathrm{e}^{\mathrm{i}\omega t}, \tag{10}$$

$$u_2^{(0)} = A_2 \sin(\gamma x_1)\cos(\varsigma x_2 + s')\mathrm{e}^{\mathrm{i}\omega t}, \tag{11}$$

where $\mathrm{i} = \sqrt{-1}$ and

$$s' = (s-1)\pi/2,$$

which includes waves either antisymmetric ($s = 1$) or symmetric ($s = 2$) in x_2, and A_1 and A_2 denote arbitrary constants.

Eqs. (10) and (11) satisfy Eqs. (8) and (9), provided

$$\begin{bmatrix} (c_{11}^* \gamma^2 + c_{66}\varsigma^2 - \rho\omega^2) & (c_{11}^* \hat{\nu} + c_{66})\gamma\varsigma \\ (c_{11}^* \hat{\nu} + c_{66})\gamma\varsigma & (c_{11}^* R\varsigma^2 + c_{66}\gamma^2 - \rho\omega^2) \end{bmatrix} \begin{bmatrix} A_1 \\ A_2 \end{bmatrix} = \begin{bmatrix} 0 \\ 0 \end{bmatrix}, \tag{12}$$

which yield non-trivial solutions when the determinant vanishes, thereby resulting in a biquadratic equation in ς of the form

$$\begin{aligned} c_{11}^* c_{66} R\varsigma^4 + [\{c_{11}^{*2} R - c_{11}^* \hat{\nu}(c_{11}^* \hat{\nu} + 2c_{66})\}\gamma^2 - \rho\omega^2(c_{11}^* R + c_{66})]\varsigma^2 \\ + (c_{66}\gamma^2 - \rho\omega^2)(c_{11}^* \gamma^2 - \rho\omega^2) = 0. \end{aligned} \tag{13}$$

For a given ω and γ, Eq. (13) yields two ς^2, i.e., $\varsigma_{(1)}^2$, $\varsigma_{(2)}^2$, each of which, from either of the linear algebraic equations denoted by the matrix equation (12), yields amplitude ratios, which may be

written in the form

$$\bar{A}_1^{(n)} = -(c_{11}^* \hat{v} + c_{66})\gamma\, \varsigma_{(n)}, \tag{14}$$

$$\bar{A}_2^{(n)} = c_{11}^* \gamma^2 + c_{66}\varsigma_{(n)}^2 - \rho\omega^2, \quad n = 1, 2. \tag{15}$$

Hence, the coupled solution functions satisfying the traction-free edge conditions at $x_2 = \pm b$ given in Eq. (7) can be written in the form

$$u_1^{(0)} = \sum_{j=1}^{2} C^{(j)} \bar{A}_1^{(j)} \sin(\varsigma_{(j)} x_2 + s')\cos(\gamma x_1)\mathrm{e}^{\mathrm{i}\omega t}, \tag{16}$$

$$u_2^{(0)} = \sum_{j=1}^{2} C^{(j)} \bar{A}_2^{(j)} \cos(\varsigma_{(j)} x_2 + s')\sin(\gamma x_1)\mathrm{e}^{\mathrm{i}\omega t}, \tag{17}$$

where $C^{(j)}$ are arbitrary constants.

The substitution first of Eqs. $(3)_2$ and (4) into Eq. (7) and then Eqs. (16) and (17) into the resulting equations yields

$$\begin{aligned} c_{11}^* \sum_{j=1}^{2} C^{(j)}(\hat{v}\gamma \bar{A}_1^{(j)} + R\varsigma_{(j)} \bar{A}_2^{(j)})\sin(\pm\varsigma_{(j)} b + s') = 0, \\ c_{66} \sum_{j=1}^{2} C^{(j)}(\varsigma_{(j)} \bar{A}_1^{(j)} + \gamma \bar{A}_2^{(j)})\cos(\pm\varsigma_{(j)} b + s') = 0, \end{aligned} \tag{18}$$

which may be written in the matrix form

$$\begin{bmatrix} (\hat{v}\gamma \bar{A}_1^{(1)} + R\varsigma_{(1)} \bar{A}_2^{(1)})\sin(\varsigma_{(1)} b + s') & (\hat{v}\gamma \bar{A}_1^{(2)} + R\varsigma_{(2)} \bar{A}_2^{(2)})\sin(\varsigma_{(2)} b + s') \\ (\varsigma_{(1)} \bar{A}_1^{(1)} + \gamma \bar{A}_2^{(1)})\cos(\varsigma_{(1)} b + s') & (\varsigma_{(2)} \bar{A}_1^{(2)} + \gamma \bar{A}_2^{(2)})\cos(\varsigma_{(2)} b + s') \end{bmatrix} \begin{bmatrix} C^{(1)} \\ C^{(2)} \end{bmatrix} = \begin{bmatrix} 0 \\ 0 \end{bmatrix}. \tag{19}$$

The linear algebraic equations in $C^{(1)}$ and $C^{(2)}$ yields non-trivial solutions when the determinant of the system vanishes. The vanishing of the determinant of the matrix equation (19) yields the dispersion curves, i.e., the ω versus γ relation, and from either of the consistent equations (18), yields amplitude ratios, which may be written in the form

$$\bar{C}^{(1)} = -(\hat{v}\gamma \bar{A}_1^{(2)} + R\varsigma_{(2)} \bar{A}_2^{(2)})\sin(\varsigma_{(2)} b + s'), \tag{20}$$

$$\bar{C}^{(2)} = (\hat{v}\gamma \bar{A}_1^{(1)} + R\varsigma_{(1)} \bar{A}_2^{(1)})\sin(\varsigma_{(1)} b + s'). \tag{21}$$

For the purpose of calculation, it is convenient to introduce the following dimensionless variables:

$$\bar{\gamma} = \frac{2b}{\pi}\gamma, \quad \bar{\varsigma} = \frac{2b}{\pi}\varsigma, \quad \bar{x}_a = \frac{\pi}{2b}x_a, \quad \bar{\Omega} = \frac{\omega}{\bar{\omega}}, \quad \bar{c}_{11}^* = \frac{c_{11}^*}{c_{66}}, \quad \tau = \bar{\omega}t, \tag{22}$$

where

$$\bar{\omega} = \frac{\pi}{2b}\sqrt{\frac{c_{66}}{\rho}}. \tag{23}$$

The substitution of Eqs. (22) and (23) yields the dimensionless form of Eq. (12) and the amplitude ratios in Eqs. (14) and (15), thus

$$\begin{bmatrix} \bar{c}_{11}^{*}\bar{\gamma}^2 + \bar{\varsigma}^2 - \bar{\Omega}^2 & (\bar{c}_{11}^{*}\hat{v}+1)\bar{\gamma}\,\bar{\varsigma} \\ (\bar{c}_{11}^{*}\hat{v}+1)\bar{\gamma}\,\bar{\varsigma} & \bar{\gamma}^2 + \bar{c}_{11}^{*}R\bar{\varsigma}^2 - \bar{\Omega}^2 \end{bmatrix} \begin{bmatrix} A_1 \\ A_2 \end{bmatrix} = \begin{bmatrix} 0 \\ 0 \end{bmatrix}, \tag{24}$$

$$\bar{A}_1^{(n)} = -(\bar{c}_{11}^{*}\hat{v}+1)\bar{\gamma}\,\bar{\varsigma}_{(n)}, \tag{25}$$

$$\bar{A}_2^{(n)} = \bar{c}_{11}^{*}\bar{\gamma}^2 + \bar{\varsigma}_{(n)}^2 - \bar{\Omega}^2, \quad n = 1, 2. \tag{26}$$

The further substitution of the dimensionless quantities defined in Eqs. (22) and (23) into Eqs. (19)–(21) yields

$$\begin{bmatrix} (\hat{v}\,\bar{\gamma}\bar{A}_1^{(1)} + R\bar{\varsigma}_{(1)}\bar{A}_2^{(1)})\sin(\pi\bar{\varsigma}_{(1)}/2 + s') & (\hat{v}\,\bar{\gamma}\bar{A}_1^{(2)} + R\bar{\varsigma}_{(2)}\bar{A}_2^{(2)})\sin(\pi\bar{\varsigma}_{(2)}/2 + s') \\ (\bar{\varsigma}_{(1)}\bar{A}_1^{(1)} + \bar{\gamma}\bar{A}_2^{(1)})\cos(\pi\bar{\varsigma}_{(1)}/2 + s') & (\bar{\varsigma}_{(2)}\bar{A}_1^{(2)} + \bar{\gamma}\bar{A}_2^{(2)})\cos(\pi\bar{\varsigma}_{(2)}/2 + s') \end{bmatrix} \begin{bmatrix} C^{(1)} \\ C^{(2)} \end{bmatrix} = \begin{bmatrix} 0 \\ 0 \end{bmatrix}, \tag{27}$$

along with the dimensionless form of the amplitude ratios in Eqs. (20) and (21)

$$\bar{C}^{(1)} = -(\hat{v}\bar{\gamma}\bar{A}_1^{(2)} + R\bar{\varsigma}_{(2)}\bar{A}_2^{(2)})\sin(\pi\bar{\varsigma}_{(2)}/2 + s'), \tag{28}$$

$$\bar{C}^{(2)} = (\hat{v}\,\bar{\gamma}\bar{A}_1^{(1)} + R\bar{\varsigma}_{(1)}\bar{A}_2^{(1)})\sin(\pi\bar{\varsigma}_{(1)}/2 + s'). \tag{29}$$

For an isotropic material,[2] the coefficients of the stiffnesses have the form:

$$c_{11}^{*} = c_{22}^{*} = E/(1-\nu^2), \quad c_{12}^{*} = \nu E/(1-\nu^2), \quad c_{66} = E/\{2(1+\nu)\}, \tag{30}$$

where E is Young's modulus and ν is the Poisson ratio. It is worth noting that the characteristic equation of the vanishing of the determinant of the matrix in Eq. (27) is a function of the Poisson ratio only for an isotropic material without referring to the specific geometry of the plate if the dimensionless quantities defined in Eqs. (22) and (23) are introduced.

In order to determine cut-off frequencies, i.e., values of ω on the $\gamma = 0$ axis, in the dispersion relations, one can examine the solutions when $\gamma = 0$. In this special case, the solutions simply degenerate, and from Eq. (12), the characteristic determinant takes the particularly simple form

$$\begin{vmatrix} c_{66}\varsigma^2 - \rho\omega^2 & 0 \\ 0 & c_{11}^{*}R\varsigma^2 - \rho\omega^2 \end{vmatrix} = 0, \tag{31}$$

which yields the two wave numbers

$$\varsigma_{(1)}^2 = \rho\omega^2/c_{66}, \quad \varsigma_{(2)}^2 = \rho\omega^2/(c_{11}^{*}R). \tag{32}$$

Under these circumstances, $A_1^{(2)} = 0$ and $A_2^{(1)} = 0$ and the resulting equations in the two homogeneous edge conditions (18) yield the characteristic determinant for the cut-off frequencies in the form

$$\begin{vmatrix} A_1^{(1)}\varsigma_{(1)}\cos(\varsigma_{(1)}b + s') & 0 \\ 0 & A_2^{(2)}\varsigma_{(2)}\sin(\varsigma_{(2)}b + s') \end{vmatrix} = 0. \tag{33}$$

[2] The analysis is performed for an orthotropic material because the solution for that symmetry is required in future work.

Therefore, two cut-off frequencies are obtained for the antisymmetric modes

$$\bar{\Omega}_n^{(1)} = 2n - 1, \tag{34a}$$

$$\bar{\Omega}_n^{(2)} = \sqrt{\bar{c}_{11}^* R}\,(2n), \quad n = 1,\ 2,\ 3,\ \ldots. \tag{34b}$$

and two for the symmetric modes

$$\bar{\Omega}_n^{(1)} = 2n, \tag{35a}$$

$$\bar{\Omega}_n^{(2)} = \sqrt{\bar{c}_{11}^* R}\,(2n - 1), \quad n = 1,\ 2,\ 3,\ \ldots. \tag{35b}$$

These cut-off frequencies provide convenient starting points for performing the calculation.

The solutions at $\bar{\Omega} = 0$ cannot be obtained from Eq. (19) in the isotropic case because then only one independent ς is obtained from Eq. (13). However, in the isotropic case the solution can be obtained by using Eq. (19) and taking the limit as $\bar{\Omega}$ approaches zero from above as in the last paragraph of Section 3 of Part 1.

Since the differential equations and the homogeneous edge conditions at the two side edges are satisfied exactly, the satisfaction of the remaining edge conditions variationally yields the result. The procedure will be explained in more detail in the next section.

4. Variational approximation

Since the solution functions given in Eqs. (16) and (17) satisfy Eqs. (6) and (7) exactly, all that remains of the variational equation (5) is

$$\int_{-b}^{b} \mathrm{d}x_2[u_b^{(0)}\delta(n_a\tau_{ab}^{(0)})]_{x_1=-l} - \int_{-b}^{b} \mathrm{d}x_2[n_a\tau_{ab}^{(0)}\delta u_b^{(0)}]_{x_1=l} = 0. \tag{36}$$

From Eqs. (16) and (17) when P dispersion curves are included, it is clear that the solution may be written in the form

$$u_1^{(0)}(\bar{x}_1, \bar{x}_2, \tau) = \sum_{p=1}^{P}\sum_{q=1}^{2}\sum_{r=1}^{2} B_{pr}\bar{H}_{1\,pq}\sin(\bar{\varsigma}_{pq}\bar{x}_2 + s')\cos(\bar{\gamma}_p\bar{x}_1 + r')\mathrm{e}^{\mathrm{i}\bar{\Omega}\tau}, \tag{37}$$

$$u_2^{(0)}(\bar{x}_1, \bar{x}_2, \tau) = \sum_{p=1}^{P}\sum_{q=1}^{2}\sum_{r=1}^{2} B_{pr}\bar{H}_{2\,pq}\cos(\bar{\varsigma}_{pq}\bar{x}_2 + s')\sin(\bar{\gamma}_p\bar{x}_1 + r')\mathrm{e}^{\mathrm{i}\bar{\Omega}\tau}, \tag{38}$$

where

$$r' = (r-1)\pi/2, \quad \bar{\varsigma}_{pq} = \bar{\varsigma}_{(q)}(\bar{\gamma}_p), \quad \bar{H}_{npq} = \bar{C}^{(q)}(\bar{\gamma}_p)\bar{A}_n^{(q)}(\bar{\gamma}_p), \quad n = 1, 2 \tag{39}$$

and the B_{pr} are arbitrary constants.

When the solution functions (37) and (38) are inserted in the variational equation (36), the resulting linear algebra uncouples into two distinct sets of linear homogeneous equations. The transcendental equations that arise when the determinant resulting from each of the uncoupled homogeneous linear algebras vanishes yield the same eigenfrequencies, which by

comparison with a PATRAN calculation is the correct frequency in each case. Consequently, a double root is always obtained from the variational equation (36). On account of this the amplitude ratios between the two uncoupled eigensolutions cannot be determined uniquely from this description.[3] Clearly, this peculiar algebraic difficulty is caused by the use of the same functional behavior in both the solution functions and the variations for the particular conditions for the cantilever, in which one edge has displacement conditions going through the variation in traction and the other edge has traction conditions going through the variation in displacement, as shown in Eq. (36).[4] Although this non-uniqueness of the amplitude ratios can be tolerated and would be removed if a forced vibration problem were treated, since it is unusual and only free vibration problems are treated in this work, it seems preferable to remove the double root and associated non-uniqueness of the amplitude ratios from the free vibration description. To this end an auxiliary constraint condition is introduced at the fixed edge. The mean displacement is taken to vanish as the constraint condition, which is introduced in the variational equation (36) by means of the method of Lagrange multipliers [6], as shown in Eq. (40). The transcendental equation resulting from Eq. (40) does not have multiple roots, and enables all the amplitude ratios to be determined. About half the roots coincide in frequency very closely with the double roots obtained from Eq. (36) and are retained and the remaining roots are spurious roots introduced by the constraint condition and are ignored.

In accordance with the foregoing discussion, the auxiliary constraint condition is introduced in Eq. (36), which takes the form

$$\int_{-b}^{b} \mathrm{d}x_2[u_b^{(0)}\delta(n_a\tau_{ab}^{(0)})]_{x_1=-l} - \int_{-b}^{b} \mathrm{d}x_2[n_a\tau_{ab}^{(0)}\delta u_b^{(0)}]_{x_1=l} + \delta\left[\lambda_{(d)}\int_{-b}^{b} \mathrm{d}x_2[u_d^{(0)}]_{x_1=-l}\right] = 0, \qquad (40)$$

where the subscript

$$d = \begin{cases} 1 & \text{for symmetric modes,} \\ 2 & \text{for antisymmetric modes} \end{cases}$$

and the undetermined Lagrange multiplier $\lambda_{(d)}$ can vary freely.

The substitution of the two-dimensional constitutive equations $(3)_1$ and (4) into Eq. (40) and the introduction of the dimensionless quantities defined in Eqs. (22) and (23) gives the

[3] The discussion in the text is for the case when the origin of co-ordinates is at the center of the cantilever, which is when the complete decoupling into two distinct sets of linear homogeneous equations occurs. If the origin is placed other than at the center of the cantilever, one set of linear homogeneous algebraic equations is obtained, but the resulting determinant does not exhibit a zero crossing and has a horizontal slope at the root, which does not yield the eigenfrequencies as accurately as when a zero crossing exists. In addition, at the eigenfrequencies the rank of the apparently fully coupled matrix is reduced by two [5] and two distinct algebraic solutions are still obtained and the amplitude ratios are not unique.

[4] Exactly the same thing happens in the case of a cantilever beam, for which an exact solution can readily be obtained, in which the amplitude ratios are uniquely determined. If the edge conditions for the beam are satisfied variationally, a double root is obtained and the amplitude ratios cannot be uniquely determined.

dimensionless form of the variational equation thus

$$\int_{-\pi/2}^{\pi/2} \mathrm{d}\bar{x}_2 \Big[[\bar{c}_{11}^{*} u_1^{(0)} \delta(u_{1,1}^{(0)} + \hat{v} u_{2,2}^{(0)}) + u_2^{(0)} \delta(u_{1,2}^{(0)} + u_{2,1}^{(0)})]_{\bar{x}_1=(-\pi l/2b)} - [\bar{c}_{11}^{*} (u_{1,1}^{(0)} + \hat{v}\, u_{2,2}^{(0)}) \delta u_1^{(0)} + (u_{1,2}^{(0)} + u_{2,1}^{(0)}) \delta u_2^{(0)}]_{\bar{x}_1=(\pi l/2b)} \Big] + \left[\delta\lambda_{(d)} \int_{-\pi/2}^{\pi/2} u_d^{(0)}\, \mathrm{d}\bar{x}_2 + \lambda_{(d)} \delta \int_{-\pi/2}^{\pi/2} u_d^{(0)}\, \mathrm{d}\bar{x}_2 \right]_{\bar{x}_1=(-\pi l/2b)} = 0, \tag{41}$$

where the spatial derivatives are taken with respect to the dimensionless co-ordinates $\bar{x}_a$.

The introduction of solution Eqs. (37) and (38) in the variational equation (41) yields a system of homogeneous algebraic equations, which may be written in the matrix form

$$\mathbf{KX} = \mathbf{0}, \tag{42}$$

where $\mathbf{K}$ is a $2P+1$ by $2P+1$ square matrix and $\mathbf{X}$ is a $2P+1$ unknown amplitude vector, which is defined by

$$X_{2(p-1)+r} = B_{pr}, \quad X_{2P+1} = \lambda_{(d)}, \tag{43}$$

from which the solution vector $\mathbf{X}$ can be readily transformed into the actual amplitude of the displacement functions and the Lagrange multiplier.

The vanishing of the determinant of $\mathbf{K}$ yields the transcendental characteristic equations for the symmetric and antisymmetric modes. The amplitude ratios may be determined from any $2P$ of the $2P+1$ equations, which are consistent when the determinant vanishes.

The amplitude ratios (43) along with the solution functions (37) and (38) yields the mode shapes of the plate for the symmetric and antisymmetric modes.

5. Discussion of results

The calculation was performed with 20 significant digit accuracy using the symbolic math package Maple [7] in quadruple precision. Since one edge is clamped and the others free (cantilevered), the modes can be categorized in accordance with the axis on the plane of the plate orthogonal to the clamped edge as (a) symmetric modes and (b) antisymmetric modes. Even though the variational equation obtained in this work is for an orthotropic material,[2] the computation was performed for an isotropic material with the Poisson ratio of 0.3 for consistency with the calculation for the out-of-plane motion of the plate in Part 1.

Fig. 2 shows the dispersion relations for the in-plane motion of a plate with two free-edges facing each other. In this figure, the dimensionless frequency $\bar{\Omega}$ is plotted against $\Re(\bar{\gamma})$ and $\Im(\bar{\gamma})$ over a range that includes the first seven complex branches near $\bar{\Omega} = 0$. Here, $\Re(\bar{\gamma})$ and $\Im(\bar{\gamma})$ represent real and imaginary, respectively.

Due to the scarcity of published results, the computed results were compared with those obtained from P3/PATRAN [8]. The same aspect ratios were chosen as those in the treatment of the out-of-plane motion of the rectangular plate in Part 1. A comparison of the results obtained from the present analysis with those from P3/PATRAN is given in Table 1.

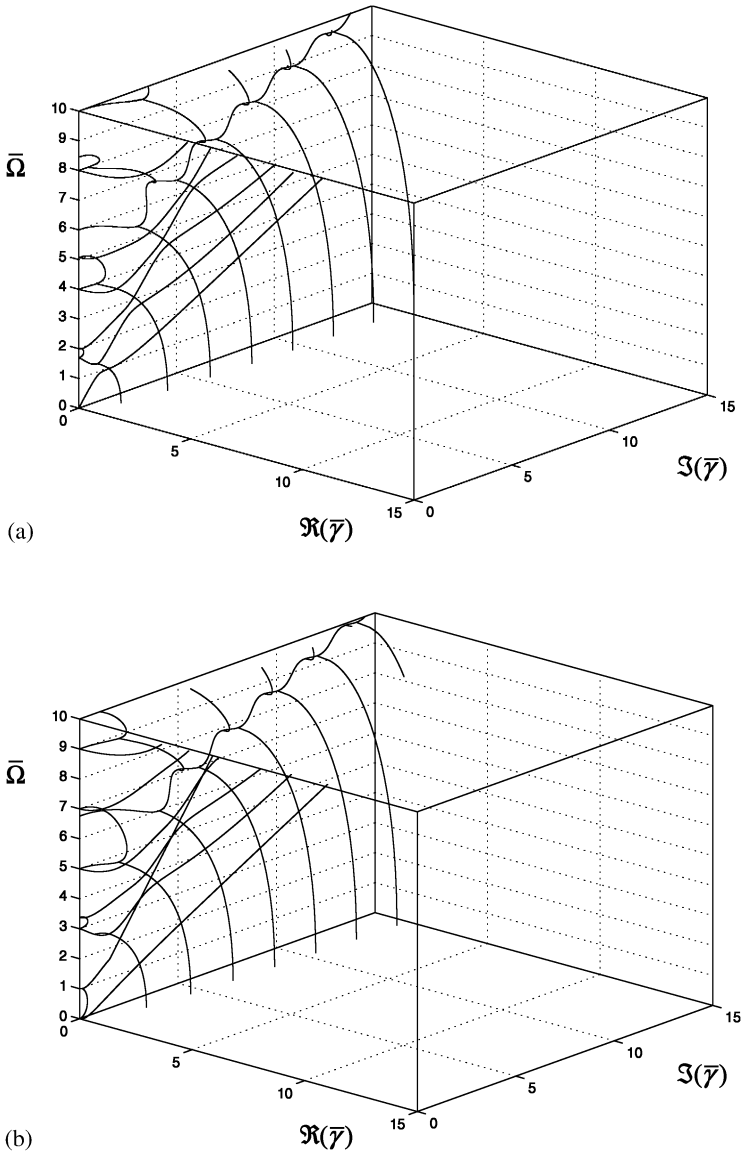

Fig. 2. Dispersion curves for the in-plane motion of the rectangular cantilever plate: (a) for symmetric modes and (b) for antisymmetric modes.

Although the results of calculations shown in Table 1 are for l/b ratios of $\frac{5}{2}$, $\frac{3}{2}$, 1, $\frac{2}{3}$ and $\frac{2}{5}$, the analysis presented in this work should not really be used for l/b ratios significantly smaller than 1 because then the edge conditions satisfied exactly are over a smaller region than those satisfied variationally. When $l/b<1$ the edge conditions at the fixed edge and the opposite free edge should be satisfied exactly and the conditions on the free opposite edges should be satisfied variationally. However, when this is done the waves that determine the dispersion become asymmetric and a much larger number of dispersion curves must be included to make any calculation. Rather than

Table 1
Dimensionless natural frequencies for the in-plane motion of the rectangular cantilever plate and their comparison with P3/PATRAN [8]

Mode #	l/b														
	2/5			2/3			1			3/2			5/2		
1	C_6	1.0849	A	C_6	0.5861	A	C_6	0.3370	A	C_6	0.1807	A	C_6	0.0749	A
	P	1.0894		P	0.5878		P	0.3382		P	0.1812		P	0.0751	
2	C_7	1.7540	S	C_7	1.2113	S	C_7	0.8102	S	C_7	0.5399	S	C_6	0.3178	A
	P	1.7522		P	1.2159		P	0.8106		P	0.5404		P	0.3194	
3	C_7	2.0990	S	C_6	1.3289	A	C_6	0.9093	A	C_6	0.5969	A	C_7	0.3236	S
	P	2.1026		P	1.3256		P	0.9081		P	0.5973		P	0.3242	
4	C_6	2.1202	A	C_7	1.5412	S	C_7	1.4452	S	C_6	1.1781	A	C_6	0.6827	A
	P	2.1178		P	1.5450		P	1.4444		P	1.1823		P	0.6850	
5	C_7	2.4042	S	C_7	1.8421	S	C_6	1.5569	A	C_6	1.3928	A	C_7	0.9560	S
	P	2.4073		P	1.8466		P	1.5602		P	1.3936		P	0.9581	
6	C_6	2.6484	A	C_6	2.0465	A	C_7	1.6541	S	C_7	1.4196	S	C_6	0.9882	A
	P	2.6511		P	2.0569		P	1.6577		P	1.4220		P	0.9922	

S: symmetric mode, A: antisymmetric mode, N( ) = natural frequency $\bar{\Omega}$ (ND) of ( ); C_n (ND) = N (current research) with n dispersion branches included, P (ND) = N (P3/PATRAN).

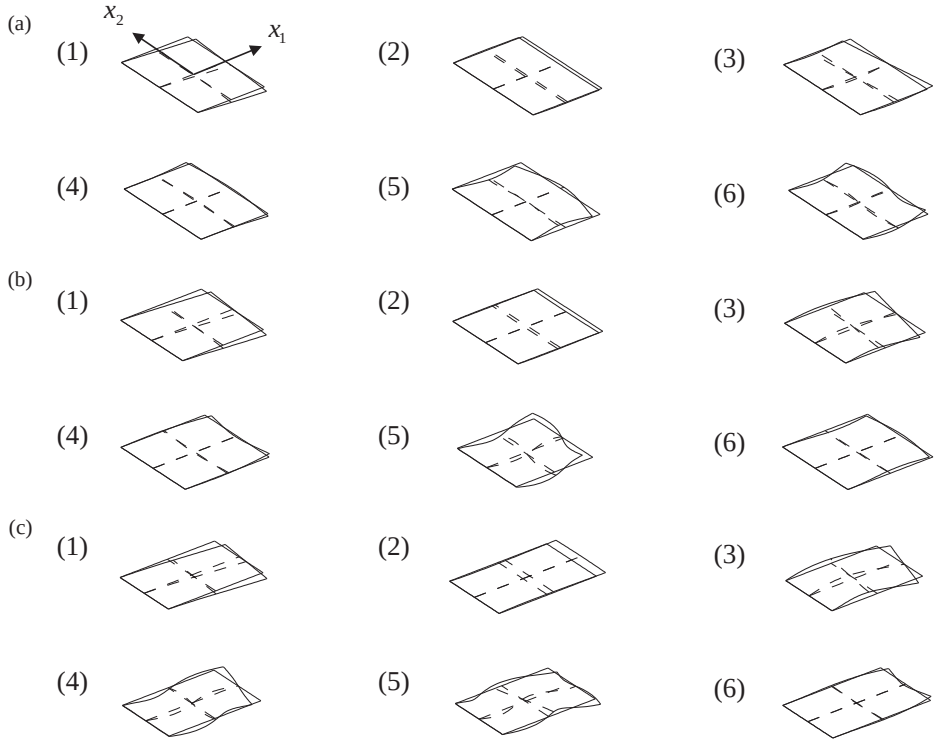

Fig. 3. First six mode shapes for the in-plane motion of the rectangular cantilever plate with various length-to-width ratios: (a) $l/b = \frac{2}{3}$, (b) $l/b = 1$, (c) $l/b = \frac{3}{2}$.

doing this additional work, the solution presented is used for ratios $l/b<1$ and it was extremely surprising to see the accuracy of the results, as shown by comparison with the FEM P3/PATRAN calculation in Table 1. That is the reason the results for $l/b<1$ are presented in the table.

Depending upon the aspect ratio of the plate, around 800–1200 quadrilateral shell elements with four nodes were also employed for the computation of the natural frequencies and the mode shapes of the plate. For the modal analysis, the subspace iteration method [8] was employed as well. With few exceptions, seven dispersion branches for the symmetric modes and six dispersion branches for the antisymmetric modes were generally included for the eigenanalysis of the present work.

Overall agreement is pretty good for most of the cases considered in this simulation. However, for the case in which the clamped edge is much wider than that of the adjacent edge, the maximum error increases up to 2%. Provided the results of the FEM are accurate enough, the error may be reduced if more branches are included.

Mode shapes of the first six modes for some selected cases are shown in Fig. 3. A little wriggling at the fixed edges is due to the fact that the boundary conditions of the clamped edge and the opposite free edge are satisfied not exactly but approximately through the minimization of the integrated virtual work induced by the displacement (or slope) of the fixed edge and the tractions on the opposite free edge.

References

[1] Y. Kobayashi, G. Yamada, S. Honma, In-plane vibration of point-supported rectangular plates, Journal of Sound and Vibration 126 (6) (1988) 545–549.
[2] N.S. Bardell, R.S. Langley, J.M. Dunsdon, On the free in-plane vibration of isotropic rectangular plates, Journal of Sound and Vibration 191 (6) (1996) 459–467.
[3] Jongwon Seok, H.F. Tiersten, H.A. Scarton, Free vibrations of rectangular cantilever plates. Part 1: out-of-plane motion, Journal of Sound and Vibration 271 (1–2) (2004) 131–146, this issue.
[4] H.F. Tiersten, Linear Piezoelectric Plate Vibrations, Plenum Press, New York, 1969.
[5] W.L. Ferrar, Algebra—A Textbook of Determinants, Matrices and Algebraic Forms, Oxford University Press, London, 1941, Chapter VIII.
[6] R. Courant, D. Hilbert, Methods of Mathematical Physics, Vol. I, Interscience, New York, 1953, Chapter IV, Section 9.2.
[7] Maple™, User Manual Release 5, Waterloo Maple Inc., 1997.
[8] P3/PATRAN™, User Manual Release 1.2, PDA Engineering-PATRAN Division, 1993.